Scholars Journal of Medical Case Reports

Abbreviated Key Title: Sch J Med Case Rep ISSN 2347-9507 (Print) | ISSN 2347-6559 (Online) Journal homepage: https://saspublishers.com **3** OPEN ACCESS

Radiology

Metastatic Melanoma of the Foot Presenting with Extensive Multi-Organ Involvement: A Radiology-Centered Case Report

EL YAAGOUBI Fatima Zohra, MD¹*, BERDAY Youssef, MD², Prof. ADNOR Said³, Prof. CHAHBI Zakaria³, Prof. WAKRIM Soukaina, MD, PhD³

DOI: https://doi.org/10.36347/sjmcr.2025.v13i10.100 | Received: 17.08.2025 | Accepted: 24.10.2025 | Published: 29.10.2025

*Corresponding author: EL YAAGOUBI Fatima Zohra, MD MD, Department of Radiology, University Hospital Souss Massa

Abstract Case Report

We report a rare case of a 24-year-old male with metastatic melanoma of the foot presenting with extensive multi-organ involvement revealed by CT imaging. The metastases involved the brain, thorax, abdomen, lymphatic system, adrenal glands, kidneys, pancreas, peritoneum, and softs tissus. Imaging showed hallmark features of melanoma, including a hyperdense brain lesion, massive pleuropulmonary mass, confluent nodal disease, and visceral organ metastases. This case highlights the importance of recognizing specific radiologic patterns of melanoma dissemination for accurate staging and treatment planning.

Keywords: Metastatic Melanoma, Foot Presenting, Radiology, Brain, Thorax, Abdomen, Kidneys.

Copyright © 2025 The Author(s): This is an open-access article distributed under the terms of the Creative Commons Attribution 4.0 International License (CC BY-NC 4.0) which permits unrestricted use, distribution, and reproduction in any medium for non-commercial use provided the original author and source are credited.

Introduction

Malignant melanoma is an aggressive cutaneous tumor with high metastatic potential, accounting for the majority of skin cancer-related deaths despite representing a small fraction of skin malignancies. Although early-stage melanoma may have a favorable prognosis, advanced disease frequently involves distant organs, including lungs, brain, liver, adrenal glands, and gastrointestinal tract. Melanoma of the foot is relatively uncommon and often associated with delayed diagnosis, increasing the risk of advanced metastatic disease.

This case presents a young male with plantar melanoma and widespread metastases, identified through contrast-enhanced CT, with emphasis on radiologic features across multiple systems. Understanding the imaging spectrum is crucial for disease staging, treatment planning, and prognosis.

CASE PRESENTATION

A 24-year-old male with a known primary cutaneous melanoma located on the plantar surface of the left foot presented for metastatic staging. The initial lesion had been biopsied three months earlier,

confirming malignant melanoma with a Breslow thickness of 4.2 mm and ulceration. Over the preceding months, the patient developed progressive exertional dyspnea, persistent left-sided chest discomfort, dry cough, fatigue, and a weight loss of approximately 10 kilograms. He also reported occasional mild headaches but denied any focal neurologic deficits, seizures, bone pain, or abdominal symptoms.

On physical examination, breath sounds were markedly reduced on the left hemithorax with dullness to percussion, suggestive of a large pleural effusion. Palpable non-tender left supraclavicular lymphadenopathy measuring about 2.5 cm was noted. Neurological examination was unremarkable. No jaundice, hepatosplenomegaly, or pedal edema was observed.

Laboratory studies revealed elevated serum lactate dehydrogenase (LDH) at 780 U/L (normal <240 U/L), S100 protein at 12.5 μ g/L (normal <0.10 μ g/L), and mildly elevated alkaline phosphatase. Liver and renal function tests were within normal limits, and there was no evidence of hypercalcemia or coagulopathy.

¹MD, Department of Radiology, University Hospital Souss Massa

²Department of Radiology, University Hospital Souss Massa

³Department of Radiology, University Hospital Souss Massa

A biopsy of the left supraclavicular lymph node was performed under ultrasound guidance. Histology revealed nests of pleomorphic epithelioid cells with prominent nucleoli and abundant cytoplasmic melanin. Immunohistochemistry was strongly positive for S100, HMB-45, Melan-A, and SOX10. Molecular testing confirmed the presence of a BRAF V600E mutation.

Contrast-enhanced CT imaging was carried out from the head to the pelvis. Non-contrast brain CT revealed a single extra-axial lesion in the left cerebellar tentorial region measuring 5.5×5.4 mm, spontaneously hyperdense (48 HU), and enhancing to 63 HU post-contrast without perilesional edema, suggestive of melanin-rich or hemorrhagic metastasis (Figure 1). No supratentorial lesions or midline shift was noted.

Thoracic imaging demonstrated a large, lobulated, intensely enhancing mass centered in the left lung and hilar region, measuring approximately $177 \times 170 \times 205$ mm. The mass caused severe narrowing of the left main bronchus (luminal stenosis >90%), engulfed the pulmonary arteries, encased the aorta and superior vena cava (SVC), and displaced the mediastinum to the right. The SVC appeared filiform, and there was compensatory dilation of the azygos vein. The mass also encased the esophagus and showed focal obliteration of the pericardial fat plane. Associated findings included a massive left-sided pleural effusion, irregular pleural thickening and nodularity (largest 15×23 mm), and a moderate pericardial effusion Figure 2).

Abdominal imaging revealed a heterogeneously enhancing right adrenal mass ($73 \times 51 \times 65$ mm) with mass effect on the inferior vena cava, and a smaller left adrenal lesion (20×14 mm) (figure 3). The left kidney contained four cortical and exophytic enhancing masses, the largest measuring 19×16 mm at the lower pole. The

right kidney displayed a larger infiltrative lesion $(28 \times 34 \times 53 \text{ mm})$ with partial loss of corticomedullary differentiation (Figure 5). The pancreas demonstrated two lesions: one in the head $(24 \times 23 \times 20 \text{ mm})$ and another in the body $(32 \times 20 \text{ mm})$ (Figure 4) with loss of fat planes and compression of the splenic vein.

Multiple bulky lymphadenopathies were observed, including interaortocaval (47 \times 53 mm), obturator internal (54 \times 32 mm), retrocaval (54 \times 43 mm), and inguinal chains. A conglomerate of peripancreatic nodes compressed adjacent structures. Several peritoneal nodules were identified, including a 38 \times 15 mm implant adjacent to the falciform ligament and others along the posterior parietal peritoneum. A right ischio-rectal mass (36 \times 28 \times 35 mm) was also seen, along with soft-tissue infiltration of the left abdominal wall musculature.

Additionally, the CT abdomen highlighted an important complication: a small bowel intussusception. This was identified on contrast-enhanced scans by the characteristic "target" and "sandwich" signs seen on axial, coronal, and sagittal planes, with a leading enlarged mesenteric lymph node acting as the pathological lead point (Figure 6).

No osseous lesions were noted on the CT scan. Based on the imaging findings, a diagnosis of extensive metastatic melanoma was established with intracranial, thoracic, abdominal, peritoneal, nodal, and soft-tissue involvement.

The patient received multidisciplinary management including supportive care and systemic therapy tailored to his advanced metastatic disease. Symptom relief measures such as drainage of the pleural effusion and close monitoring were also implemented.



Figure 1: Three contrast-enhanced brain CT scans in the parenchymal window, including axial, coronal, and sagittal views, demonstrate an extra-axial, well-defined, oval-shaped left paramedian infratentorial lesion, hyperdense with contrast enhancement and no surrounding edema, consistent with a cerebellar metastasis

EL YAAGOUBI Fatima Zohra et al, Sch J Med Case Rep, Oct, 2025; 13(10): 2603-2607



Figure 2: Contrast-enhanced thoracic CT scans in the venous phase, including axial, coronal, and sagittal views, reveal a large pleuro-pulmonary mass on the left side with irregular, lobulated contours and heterogeneous intense enhancement, causing significant mass effect and mediastinal shift, consistent with a pleuro-pulmonary metastasis



Figure 3: Contrast-enhanced abdominal CT scans in the venous phase, including axial, coronal, and sagittal views, show a well-defined, heterogeneous right adrenal lesion with areas of hypodensity and intense enhancement, exerting mass effect on adjacent structures, consistent with an adrenal metastasis

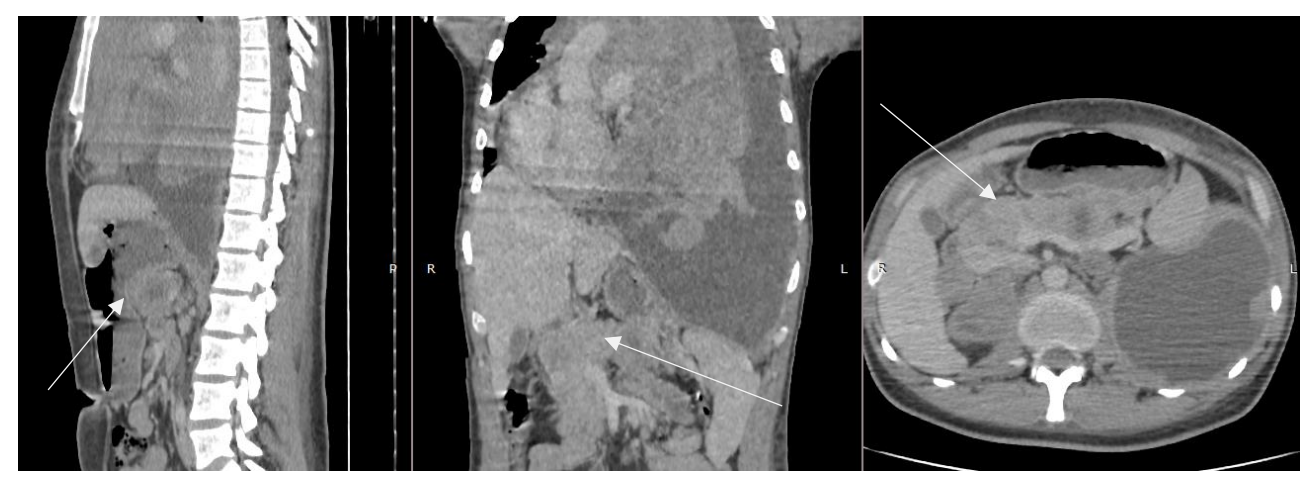


Figure 4: Contrast-enhanced abdominal CT scans in the venous phase, including axial, coronal, and sagittal views, reveal multiple pancreatic lesions of varying density and enhancement patterns, with irregular contours and loss of fat planes adjacent to vascular structures, indicative of pancreatic metastases

EL YAAGOUBI Fatima Zohra et al, Sch J Med Case Rep, Oct, 2025; 13(10): 2603-2607



Figure 5: The contrast-enhanced abdominal CT scan in the venous phase, with axial, coronal, and sagittal reconstructions, reveals several irregular, enhancing masses in the right kidney, indicative of metastatic lesions.

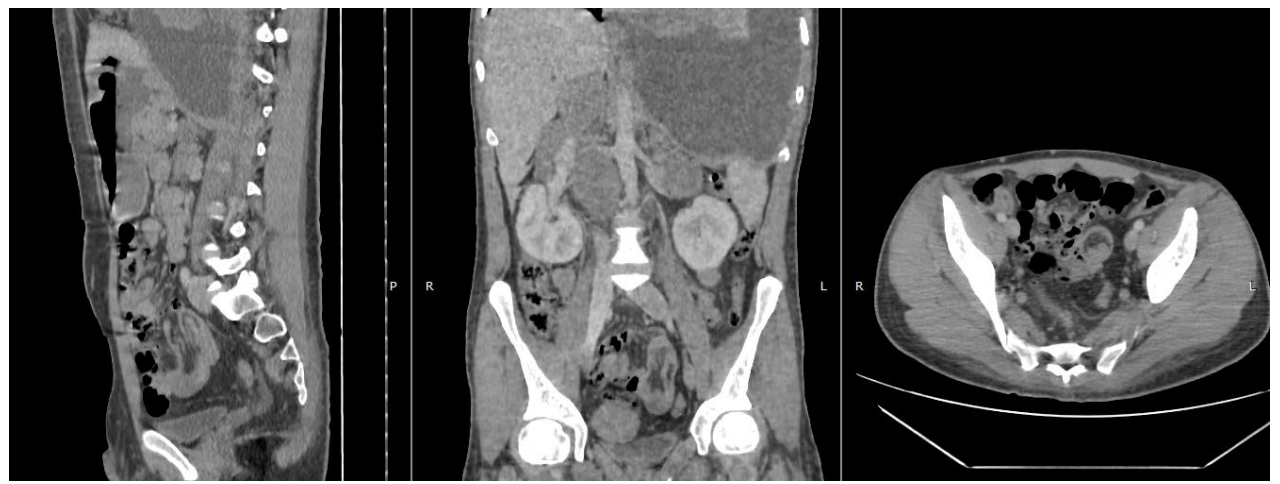


Figure 6: Contrast-enhanced abdominal CT in axial, coronal, and sagittal planes demonstrates a classic "target" and "sandwich" sign consistent with small bowel intussusception, with a leading point corresponding to an enlarged mesenteric lymph node

DISCUSSION

Imaging plays a pivotal role in the staging and management of metastatic melanoma, particularly given the tumor's aggressive nature and wide metastatic potential [1]. Each imaging modality offers distinct advantages and limitations which are crucial for comprehensive evaluation [2].

Ultrasound is frequently the first-line modality for superficial lymph nodes and accessible soft tissue lesions, as well as guidance for biopsies. In this patient, ultrasound allowed precise localization and sampling of the left supraclavicular lymphadenopathy. High-resolution ultrasound can distinguish benign from malignant nodes by features such as size, shape, border definition, internal architecture, and vascular pattern with Doppler imaging [3].

Computed Tomography (CT) remains the cornerstone for systemic staging. Its rapid acquisition and excellent spatial resolution facilitate detection of thoracic, abdominal, and pelvic metastases. In melanoma, CT typically reveals hypervascular soft tissue masses that avidly enhance post-contrast, as seen with

the large mediastinal mass and visceral organ lesions in this case. CT is particularly sensitive for detecting lung nodules, lymphadenopathy, adrenal lesions, and pleural abnormalities [4]. The identification of vascular encasement, bronchial stenosis, and mass effect on mediastinal structures underscores the aggressive local invasion. For brain imaging, non-contrast CT can detect hyperdense hemorrhagic or melanin-rich metastases but lacks sensitivity for smaller or non-hemorrhagic lesions [5].

Magnetic Resonance Imaging (MRI) is the modality of choice for brain and soft tissue metastases due to its superior soft tissue contrast. Melanotic melanoma metastases classically appear hyperintense on T1-weighted images and hypointense on T2-weighted sequences because of paramagnetic melanin content and often show heterogeneous enhancement after gadolinium administration (5). MRI is essential for detecting leptomeningeal disease and characterizing cerebellar or brainstem lesions where CT sensitivity is limited. For abdominal organs, MRI provides better tissue characterization of indeterminate lesions, especially liver and pancreas, and aids in differentiating cystic from solid masses [6].

Positron Emission Tomography—Computed Tomography (PET-CT) using 18F-FDG is highly valuable in melanoma staging, detecting metabolically active disease even in normal-sized nodes or occult metastases, and assessing treatment response [7]. PET-CT can identify subclinical metastases, improve sensitivity over conventional imaging, and guide biopsy. However, it is less useful for brain metastases due to high background glucose metabolism in the brain and may miss very small lesions.

Other advanced techniques, including contrastenhanced ultrasound and diffusion-weighted imaging (DWI) MRI, have been explored to improve detection and characterization of melanoma metastases, especially in softs tissus and lymph nodes [8].

The multi-organ metastatic pattern seen here reflects melanoma's hematogenous and lymphatic spread. Bilateral adrenal and renal metastases are hallmark findings indicating advanced disease. Pancreatic involvement is less common but should raise suspicion in the setting of widespread metastasis. The presence of peritoneal implants and soft tissue masses in unusual locations like the ischio-rectal fossa highlights the need for whole-body imaging to capture the full disease burden.

In conclusion, integration of imaging modalities—starting with ultrasound-guided biopsy, followed by contrast-enhanced CT for systemic evaluation, supplemented by MRI for CNS and soft tissue assessment, and PET-CT for metabolic mapping—offers a comprehensive approach to staging

CONCLUSION

This case illustrates the diverse and aggressive metastatic behavior of melanoma, particularly in a young patient. Radiologists should be vigilant in identifying uncommon metastatic sites. The constellation of findings, including bulky pleuropulmonary mass, nodal coalescence, multiorgan visceral involvement, and peritoneal seeding, are highly suggestive of advanced melanoma. CT remains a pivotal modality in the initial staging and monitoring of treatment response.

REFERENCES

- 1. Ferlay J, et al. Global Cancer Observatory: Cancer Today. Lyon, France: International Agency for Research on Cancer; 2020.
- 2. Diepgen TL, Mahler V. The epidemiology of skin cancer. Br J Dermatol. 2002;146(Suppl 61):1–6.
- 3. Riker AI, Zea N, Trinh T. The epidemiology, prevention, and detection of melanoma. Ochsner J. 2010;10(2):56–65.
- 4. Nelson KC, Tsao H. Melanoma and genetics. Clin Dermatol. 2009;27(1):46–52.
- 5. Disibio G, French SW. Metastatic patterns of cancers: results from a large autopsy study. Arch Pathol Lab Med. 2008;132(6):931–939.
- 6. Deneve JL, Messina JL, Marzban SS, Gonzalez RJ. Lymphadenectomy in melanoma: current controversies. Hematol Oncol Clin North Am. 2014;28(3):465–479.
- 7. Gore ME, Lorigan P, Gurney H, et al. Treatment of metastatic renal cancer with high-dose intravenous interleukin-2: the Royal Marsden Hospital experience. Br J Cancer. 1995;71(6):132–136.
- 8. Young SE, Martinez SR, Young MJ. The diagnosis and management of metastatic melanoma. Surg Clin North Am. 2014;94(5):1049–1076.